Available online at www.sciencedirect.com
SCIENCE DIRECT®
Tetrahedron: *Asymmetry* 15 (2004) 537–543
Tetrahedron: *Asymmetry*

Cyclic diphenic hydrazide: crystal structure, resolution, absolute configuration, and enantiomerization pathway investigation

Denis A. Lenev,[a,*] Konstantin A. Lyssenko,[b] Denis G. Golovanov,[b] Oliver Weingart,[c] Volker Bußc and Remir G. Kostyanovsky[a]

[a]*N.N. Semenov Institute of Chemical Physics, Russian Academy of Sciences, 4 ul. Kosygina, 119991 Moscow, Russia*
[b]*A.N. Nesmeyanov Institute of Organoelement Compounds, Russian Academy of Sciences, 28 ul. Vavilova, 119991 Moscow, Russia*
[c]*Institute of Chemistry, Universität Duisburg-Essen, Lotharstrasse 1, D-47048 Duisburg, Germany*

Received 31 October 2003; accepted 2 December 2003

Abstract—Two isomorphous crystal structures of inclusion compounds of the racemic cyclic monohydrazide of diphenic acid (6,7-dihydro-dibenzo[*d*,*f*][1,2]diazocine-5,8-dione) **1** with EtOH and MeCN are reported. In the crystals with space group *C*2/*c* the axially chiral enantiomers strictly alternate, forming zigzag tapes with an $R_2^2(8)$ H-bonding graph. (+)-**1** was obtained by partial crystallization of the diastereomeric prolinomethyl derivatives **2** followed by acid cleavage of the auxiliary. The (*R*)-configuration of (+)-**1** was established from the crystal structure of (*R*,*S*,*S*)-$(+)_{366}$-**2**. The free activation energy for enantiomerization of **1** at 373 K was determined as $\Delta G^{\ddagger} = (126.7 \pm 0.8)$ kJ mol^{-1}. The enantiomerization pathway was investigated using quantum-mechanical methods. At the DFT B3LYP/6-31G(d,p) level two enantiomeric C_2-symmetric transition states and two enantiomeric pathways were found, with a calculated barrier of 155.6 kJ mol^{-1}. The pathways can be divided into two steps, one involving primarily inversion of the amidic bridge, the other movement of the aromatic rings. CD-spectra of (*R*)-**1** agree with previously published data on twisted biphenyls.

1. Introduction

Molecules with axial chirality have attracted attention recently because of their frequent occurrence in nature[1,2] and their numerous applications in asymmetric synthesis, catalysis,[3–6] and enantiomeric resolutions.[7] The enantiomerization barrier is often low, which leads to fascinating effects such as chiral symmetry breaking in crystallization of 1,1′-binaphtyl[8] or, more recently, in a whole family of atropoisomeric biaryls.[9]

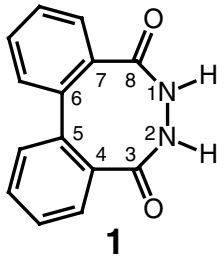

1

Interest has focussed also on conformationally restricted axially chiral molecules like 2,2′-bridged 1,1′-biaryls. Their enantiomerization behavior,[10–13] chiroptical properties,[14–16] and supramolecular potential[17,18] have been the subject of several investigations. In the course of our studies of crystal engineering using chiral C_2-symmetric bicyclic bis-lactams,[19,20] we were attracted by a simple heterocycle with two *cis*-amidic groups, the cyclic monohydrazide of diphenic acid **1**.[21] NMR studies of derivatives of **1**[22] indicate that this molecule, due to the rigidity of conjugated fragments and steric demands, should exist in a chiral C_2-symmetric conformation with significant configurational stability. Our work aims at elucidating the conformation, configuration, and solid state H-bonding capabilities of **1**, which may also be important for understanding the biological (analgesic) activity of its homologues.[23,24]

2. Results and discussion

2.1. Synthesis and resolution

Racemic (±)-**1** was synthesized from diphenic anhydride using one of the methods of Labriola[21] with minor modifications in 10% total yield (Scheme 1). Single

* Corresponding author. Tel.: +7-095-9397245; fax: +7-095-9382156; e-mail: linya@inbox.ru

0957-4166/$ - see front matter © 2003 Elsevier Ltd. All rights reserved.
doi:10.1016/j.tetasy.2003.12.003

crystals were grown from ethanol[21] and acetonitrile solutions and examined by X-ray diffraction (XRD).

To obtain enantiomeric **1** the readily available chiral derivatizing agent, (*S*)-(−)-*N*-(methoxymethyl)proline methyl ester,[25] was employed, which converts racemic **1** into the prolinomethylated derivatives **2**. Of these only one, the $(+)_{366}$-diastereomer, crystallizes from acetonitrile. Single crystals of the diastereomer were grown from ethyl acetate and subjected to an XRD analysis. The absolute configuration of the biphenyl moiety was (*R*). Subsequent acidic workup of (*R*,*S*,*S*)-$(+)_{366}$-**2** lead to (*R*)-(+)-**1** with >90% ee according to NMR analysis.

The enantiomerization barrier of **1** was determined (see experimental section) in acetonitrile at 373 K as $\Delta G^{\ddagger} = (126.7 \pm 0.8)\,\mathrm{kJ\,mol^{-1}}$.

2.2. Crystal structure analysis

Crystallographic data for **1** and **2** are presented in Table 1.

2.2.1. Compound (±)-1. (±)-**1** forms isomorphous inclusion compounds with MeCN and EtOH (Table 1). The density of the ethanol solvate is higher than that of the acetonitrile solvate, with cell dimensions of both being very close to each other. The H-bonding network in both structures (Fig. 1) is typical for racemic chiral dilactams in that the heterocyclic molecule forms H-bonded centrosymmetric zigzag tapes with $R_2^2(8)$[26] eight-membered rings and strictly alternating enantiomers.[17,19,20,27] The host molecule occupies a general position with C_1 symmetry while the guest molecules (not shown in Fig. 1) in both structures are disordered by the center of symmetry and located in the cavities (approximately $4.1 \times 7.3 \times 9.7$ Å in size) between the adjacent H-bonded rings. Despite the formation of weak O–H···O=C hydrogen bonds in the case of the ethanol solvate the supramolecular organization including the geometry of the N–H···O bonds remains practically the same, indicating the stability of the zigzag motif.

Bond lengths, bond angles, and torsion angles for **1**·½MeCN together with **2** and the corresponding DFT-calculated values for the ground state and the transition state for enantiomerization of **1** are given in Table 2. The principal geometrical parameters of the host molecules **1** in the two solvates are identical within the experimental error, the maximum variation of 1° being observed for the C(8)–N(1)–N(2)–C(3) torsion angle.

Both the N–N bond length (1.393 Å) and the C(8)–N(1)–N(2)–C(3) torsion angle (93.8°) are close to the values found in acyclic 1,2-dibenzoylhydrazine (1.385 Å and 104.23°, respectively).[28] The two N–H···O hydrogen bonds are nonequivalent (2.837 and 2.898 Å) and typical for this kind of interaction. The dihedral angle C(4)–C(5)–C(6)–C(7) [63.7 for the (*S*)-enantiomers of the tape] characterizes the twist of the biphenyl core and is important for both the circular dichroism study and the enantiomerization reaction.

2.2.2. Compound (*R*,*S*,*S*)-$(+)_{366}$-2. The crystal structure of (*R*,*S*,*S*)-$(+)_{366}$-**2** is depicted in Figure 2. With the known (*S*)-configuration of the prolinomethyl residue it is possible to assign the unknown configuration of the biphenyl core as (*R*). Perusal of Table 2 reveals that bond lengths and bond angles of the eight-membered

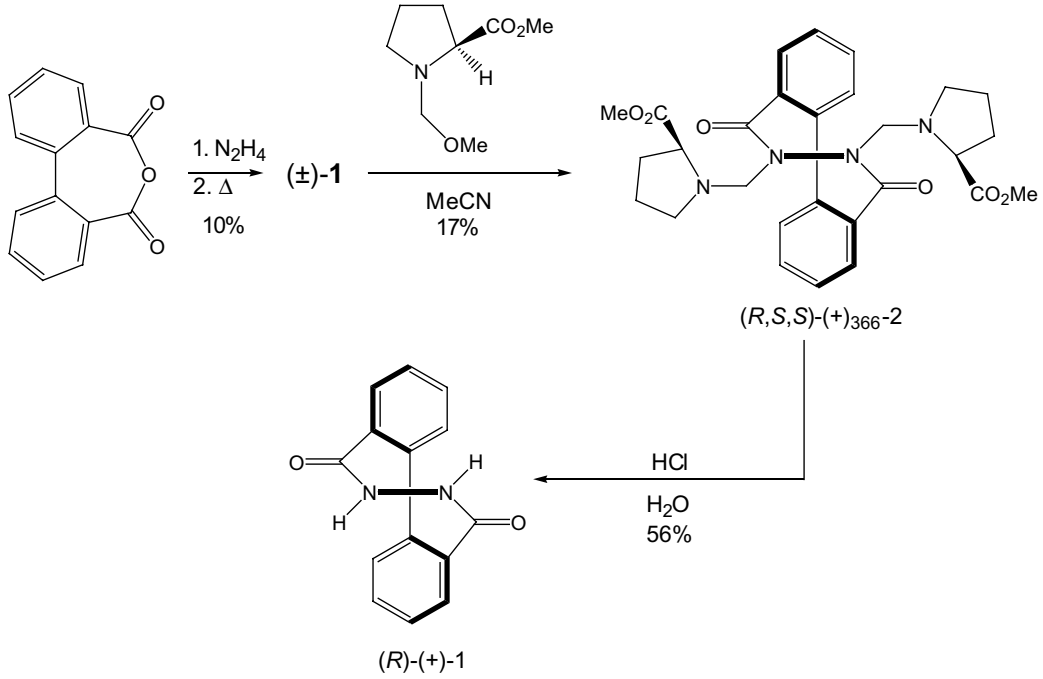

Scheme 1. Synthesis of racemic and enantiomeric **1**.

Table 1. Crystallographic data for (±)-**1** and (*R*,*S*,*S*)-(+)$_{366}$-**2**

	(±)-**1**		(*R*,*S*,*S*)-(+)$_{366}$-**2**
Formula	$C_{14}H_{10}N_2O_2\,\frac{1}{2}CH_3CN$	$C_{14}H_{10}N_2O_2\,\frac{1}{2}C_2H_5OH$	$C_{28}H_{32}N_4O_6$
T, K	110		298
Crystal system	Monoclinic		Monoclinic
Space group	$C2/c$		$P2_1$
a, Å	16.738(4)	16.691(4)	7.8070(16)
b, Å	7.359(2)	7.280(2)	15.820(3)
c, Å	20.408(4)	20.320(4)	11.044(2)
β, °	90.138(6)	90.139(6)	105.84(3)
V, Å^3	2513.7(10)	2469.0(10)	1312.2(5)
Z	8		2
M	258.77	261.27	520.58
μ(MoK$_\alpha$), cm^{-1}	0.93	0.98	11.07
F(0 0 0)	1080	1096	1476
D_{calcd}, g cm^{-3}	1.368	1.406	2.023
$2\theta_{max}$, °	50	54	56
Diffractometer	Smart CCD		Siemens P3/PC
Scan mode	ω		$\theta/2\theta$
No. of reflections measured	6809	9934	3530
No. of independent reflections	2188	2893	3307
No. of reflections with $I > 2\sigma(I)$	1339	2391	1924
No. of parameters	195	230	345
R_{int}	0.0502	0.0212	0.0277
R_1	0.0524	0.0529	0.0614
wR_2	0.1270	0.1386	0.1366
GOF	1.084	1.089	1.068
Max/min peak, e Å^{-3}	0.161/−0.159	0.634/−0.634	0.15/−0.22

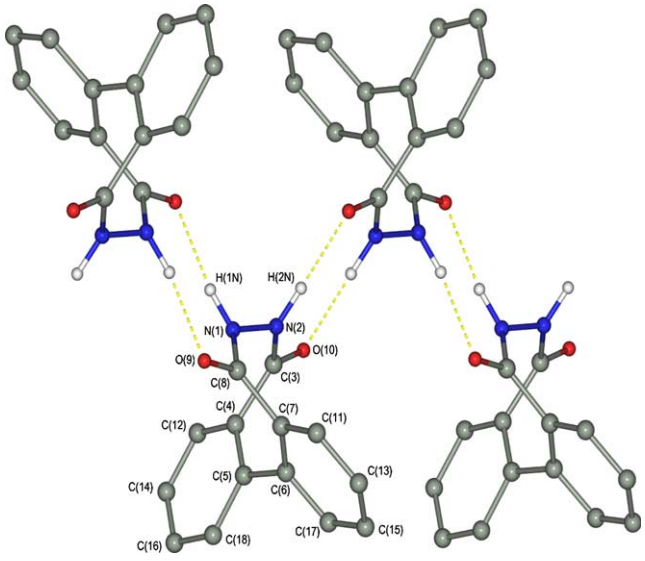

Figure 1. Centrosymmetric zigzag tapes and atom numbering in the crystal structure of (±)-**1**.

diazocine heterocycle are close to the corresponding values of **1**. As a geminal NCH_2N system **2** could exhibit stereoelectronic n–σ* interaction. However, in the crystal structure there is no evidence for this, such as an antiperiplanar geometry of the amine nitrogen lone pairs with respect to the NCH_2 bonds, which is missing also in the previously studied prolinomethylated chiral glycouril.[29]

2.3. UV and CD spectra

The UV spectrum of *R*-(+)-**1** (not shown) has an absorption maximum at 202 nm in methanol and in acetonitril and two shoulders at 270 and 235 nm, while the CD spectrum (Fig. 3) exhibits two positive bands around 240 and 220 ($\Delta\varepsilon$ 30 and 42, respectively) and negative absorbance below 200 nm. There are no significant solvent and temperature effects on these spectra. Empirical rules have been derived by Mislow et al. and Suzuki[14–16,30] for the ORD and CD spectra of bridged biaryls, which are supported by theoretical calculations by Sandström and Rashidi-Ranjbar.[31] Following these rules we assign the long wavelength positive band at 240 nm of (+)-**1** to the A-band of a negatively twisted biphenyl unit (angle of twist $-90° < \theta < 0°$). Moreover, the high energy positive band at 220 and the negative CD-absorbance below 200 nm correlate in magnitude and shape to bands observed in an (*R*)-configurated bridged biphenyl derivative.[15] Both assignments agree with the configuration for (+)-**1** derived from the X-ray analysis of **2** as being (*R*). For an in-depth analysis of the electronic spectra of **1**, especially the possible role of the two amide groups, we refer to on-going calculations in our laboratories, which will be reported elsewhere.

2.4. Enantiomerization pathway

All calculations (geometry optimizations, frequency calculations, and reaction path following) were performed with the DFT Becke3LYP method and the 6-31G(d,p) basis set, as provided by the GAUSSIAN98

Table 2. Main structural parameters of **1** and **2** and DFT-calculated values for **1** (bond lengths in Å, bond and torsion angles in deg)

Bond[a]	**1**[b]	(*R*,*S*,*S*)-**2**	(*S*)-**1** GS[c]	(*S*)-**1** TS[d]
N(1)–N(2)	1.393(3)	1.402(2)	1.380	1.437
N(2)–C(3)	1.349(3)[e]	1.363(5)[e]	1.382	1.413
C(3)–C(4)	1.489(3)[e]	1.507(6)[e]	1.498	1.503
C(3)–O(10)	1.229(3)[e]	1.213(5)[e]	1.220	1.221
C(4)–C(5)	1.400(3)[e]	1.397(5)[e]	1.412	1.425
C(5)–C(6)	1.496(3)	1.496(5)	1.500	1.517
$\sum_N$[f]	356.1	359.5	357.8	334.1
C(8)–N(1)–N(2)–C(3)	93.8	−83.9[d]	98.3	−116.7
C(4)–C(5)–C(6)–C(7)	63.7	−58.6[d]	67.4	58.5

[a] Numbering according to Figure 1.
[b] For the (*S*)-enantiomer in the racemic tape.
[c] Ground state for enantiomerization; DFT calculated results (see below).
[d] Transition state for enantiomerization; DFT calculated results (see below).
[e] Average of the two values of nonequivalent groups in the C_1-symmetric molecules.
[f] Denotes the sum of the three bond angles at the amidic nitrogen atom.

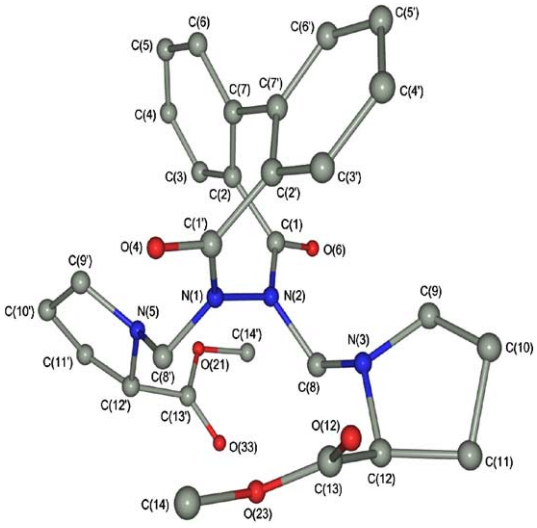

Figure 2. Crystal structure of the (R,S,S)-$(+)_{366}$-**2**.

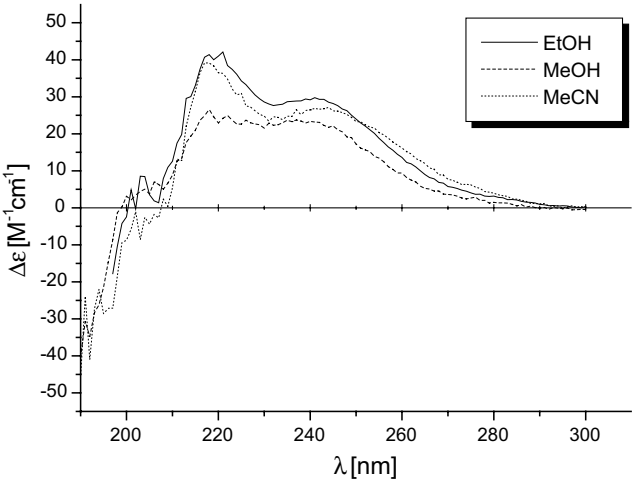

Figure 3. CD spectra of (+)-**1** in different solvents.

set of routines.[32] The structure of **1** was optimized with C_2 symmetry constraints applied. The resulting bond lengths and angles correspond close to the X-ray data of **1** and of its non-H-bonded derivative **2** (Table 2). The C_2-symmetric transition state (TS) of the enantiomerization reaction was found using the STQN algorithm. It was further characterized as a first order saddle point by calculation of the second derivatives with respect to the atomic coordinates (frequencies). By optimizing the reaction coordinate in internal mass-weighted coordinates we found that from the TS the reaction path leads directly to the (*S*)- and to the (*R*)-enantiomer (Fig. 4). To compare the calculated data with the experimental result the frequencies were scaled by 0.9806,[33] in order to obtain the zero-energy-corrected thermal energy at 373 K. From this a barrier to enantiomerization of 155.6 kJ mol^{-1} was calculated, which is in fair agreement with the experimental value. Whereas in the ground state the amidic nitrogen is almost planar (see corresponding entry in Table 2) there is significant pyramidalization in the TS, which indicates loss of amidic resonance and is one of the factors contributing to the calculated energy difference.

Figure 4 shows that the energy profile of the reaction is asymmetric: from the TS toward the (*S*) enantiomer there is a steep descent, toward the (*R*) minimum it is rather flat. This asymmetry is not accidental. The C_2 symmetry of the TS implies that there are two its enantiomers, (*S*) and (*R*) (configuration derived from biphenyl chirality) in the potential energy surface of the system. These TSs connect the (*S*)- and (*R*)-forms of **1** by two pathways, which are mirror-image forms of each other. From the data shown in Table 2 it is evident that in going from (*S*)-**1** to the (*S*)-TS the change of the biphenyl twist is significantly smaller than the change of the bis-amide bridge, 9° versus −215°. Going from the (*S*)-TS to the (*R*)-**1** enantiomer the conditions are reversed: now the biphenyl twist angle has to change by 130° and the bis-amide angle by only −18°, to reach the inverted dihedral angles of this enantiomer of −67.4° and −98.3°, respectively. It is thus quite obvious that the inversion about the two bonds proceeds in consecutive steps. This is graphically displayed in Figure 5 where the change of the two dihedral angles is plotted as a function of the progress of the reaction.

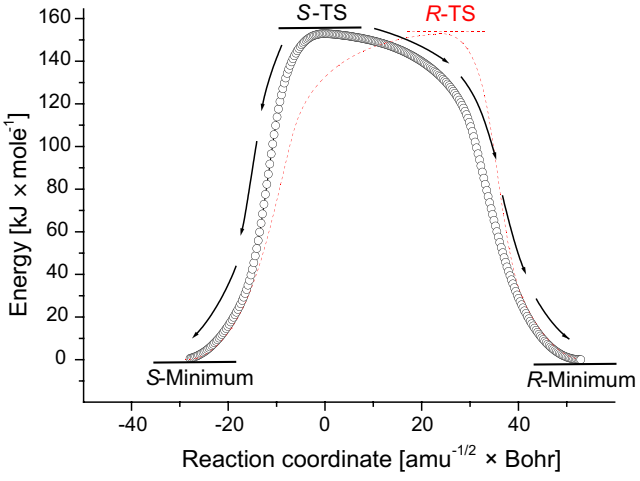

Figure 4. Reaction paths leading from the (*S*)-transition state of epimerization of **1** to the (*R*)- and the (*S*)-enantiomers arrows indicating the directions followed. The dashed line denotes the enantiomeric pathway via the (*R*)-transition state (schematically).

Enantiomeric transition states of enantiomerization reactions are not uncommon[10,34] and have been discussed in general by Salem.[35]

3. Conclusion

The cyclic hydrazide of diphenic acid **1** was obtained in enantiomerically pure form by crystallization of the prolinomethylated derivative (*R*,*S*,*S*)-(+)$_{366}$-**2** and subsequent cleavage of the chiral auxiliary. The absolute configuration of the (+)-enantiomer was unambiguously determined by single crystal X-ray diffraction analysis of (*R*,*S*,*S*)-(+)$_{366}$-**2** with the known absolute configuration of the proline. We assign the band at 240 nm in the CD spectrum of (*R*)-(+)-**1** (shoulder in the UV) to Suzuki's A-band at 240 nm, with the positive sign in agreement with Mislow's rule for the negative biphenyl twist angle. The enantiomerization pathway of **1** was studied at the DFT Becke3LYP/6-31G(d,p) level of quantum theory. The reaction was found to proceed in two steps, one occurring before the transition state and involving mainly amide bridge inversion, the other one later and leading to inversion of the biphenyl entity. The transition state was found to be chiral C_2-symmetric. From this we conclude that there are two enantiomeric transition states and two enantiomeric reaction paths, which require a statistical factor of 2 in the Eyring calculation of the racemization kinetics. The experimental free energy of activation (126.7 ± 0.8 kJ mol^{-1} at 373 K) and the calculated barrier (155.6 kJ mol^{-1}) are in fair agreement.

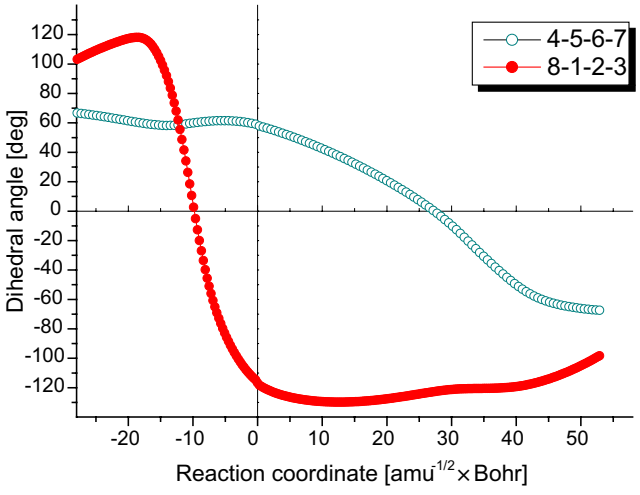

Figure 5. Change of the biphenyl C(4)–C(5)–C(6)–C(7) and the bisamide C(8)–N(1)–N(2)–C(3) dihedral angles during the enantiomerization reaction of **1**.

Racemic (±)-**1** forms inclusion compounds with ethanol and acetonitrile, with the host H-bonding network typical for chiral dilactams consisting of centrosymmetric zigzag tapes with an $R_2^2(8)$ H-bonding graph. We were unable to grow single crystals of the enantiomeric **1**, a problem already encountered in similar systems.[17] This should not be an obstacle to use this molecule in supramolecular chemistry and for crystal engineering, for example, to synthesize chiral quasiracemates based on the core of cyclic diphenic hydrazide (cf. Ref. 36). Moreover, homologues of the title compound possess analgesic activity in mice[23] and this study may be helpful in elucidating its mechanism.

4. Experimental

Elemental analyses were performed in the Microanalyses laboratory of the Institute of Organic Chemistry of Russian Academy of Sciences, Moscow, Russia. Melting points are uncorrected. MeCN was distilled from CaH_2 and stored over 3 Å molecular sieves. Analytical thin-layer chromatography was performed on Merck polymer-backed pre-coated plates (0.2 mm). NMR ^{1}H and ^{13}C spectra were recorded on a Bruker WM-400 spectrometer at 400.13 MHz for ^{1}H and 100.61 MHz for ^{13}C, using TMS or residual ^{1}H signal of solvents as an internal reference in proton spectra and solvent C signal in carbon spectra. Optical rotations were measured on a Polamat A instrument (cell length 0.05 m). CD spectra were recorded on AVIV 62A DS (**1**) and Jasco J-500A (**2**) instruments.

Crystallographic data for (±)-**1**·½MeCN, (±)-**1**·½EtOH and (*R*,*S*,*S*)-(+)$_{366}$-**2** are presented in Table 2. The structures were solved by direct methods and refined by full-matrix least-squares against F^2 in the anisotropic (H-atoms isotropic) approximation, using the SHELXTL-97 package. The analysis of the electron Fourier difference synthesis revealed that guest solvent molecules in **1** are disordered by the center of symmetry in two (MeCN) and four (EtOH) positions with equal occupancy. The positions of hydrogen atoms in **1** were calculated and included in the refinement in the riding model approximation. CCDC entries 223050 (**1**·½MeCN), 225178 (**1**·½EtOH) and 223051 (**2**) contain

the supplementary crystallographic data for this paper. These data can be obtained free of charge at www.ccdc.cam.ac.uk/conts/retrieving.html [or from the Cambridge Crystallographic Data Centre, 12, Union Road, Cambridge CB2 1EZ, UK; fax: (internat.) +44-1223/336-033; e-mail: deposit@ccdc.cam.ac.uk].

All calculations were performed in the Computing center of the University Duisburg-Essen on HP/Convex V2250 computer.

4.1. Diphenic hydrazide (±)-1 (6,7-dihydro-dibenzo[*d*,*f*]-[1,2]diazocine-5,8-dione)

Diphenic anhydride[37] (1.01 g, 4.5 mmol) was dissolved in hot MeCN (30 mL) and to this solution was quickly added a solution of anhydrous N_2H_4 (156 mg, 4.9 mmol) in MeCN (1 mL). After several hours white crystals of diphenic monohydrazide started to precipitate. The precipitate (658 mg, mp 174–176 °C, ^{1}H NMR (CD_3OD) δ, ppm, J, Hz: 7.17 (t, $^3J = 7.2$, 2H), 7.44 (m, 5H), 7.83 (d, $^3J = 7.2$, 1H)) was filtered, washed with MeCN and used without purification. It was heated at 220–300 °C at 20 mmHg for 3 h in a sublimator. The sublimate (230 mg) was recrystallized from MeCN. The product crystallized in massive blocks (yield 106 mg, 9.9% from diphenic anhydride), mp 310–311 °C. ^{1}H NMR (DMSO-d_6) δ, ppm, J, Hz: 2.05 (MeCN, s, 1.5H), 7.28 (d, $^3J = 8$, 2H), 7.48 (d, $^3J = 7.2$, 2H), 7.54 (m, 4H), 9.99 (s, 2H, 2NH). ^{13}C NMR (DMSO-d_6) δ, ppm: 126.46, 128.57, 129.87, 130.38, 134.25, 136.70, 173.11. Anal. Calcd for $C_{14}H_{10}N_2O_2\,\frac{1}{2}CH_3CN$ (M 258.77) (%): C, 69.62; H, 4.48; N, 13.53. Found (%): C, 69.73; H, 4.39; N, 13.41. ^{1}H NMR spectrum (DMSO-d_6) of the crystals grown from ethanol has shown the presence of a half-molar quantity of EtOH.

4.2. (2*S*)-2-Pyrrolidinecarboxylic acid, 1-[[7,8-dihydro-7-[[(2*S*)-2-(methoxycarbonyl)-1-pyrrolidinyl]methyl]-(*R*)-5,8-dioxodibenzo[*d*,*f*][1,2]diazocin-6(5*H*)-yl]methyl]-, methyl ester (*R*,*S*,*S*)-(+)$_{366}$-2

(±)-**1** (494 mg, 2.08 mmol) and (*S*)-(−)-*N*-(methoxymethyl)proline methyl ester (720 mg, 4.16 mmol) were mixed in MeCN (1 mL) and refluxed until the solid was fully dissolved. The color of the solution changed from colorless to yellow to pink. After 24 h at 20 °C the resulting suspension consisted of two types of crystals: massive yellowish prisms and white powder. These crystals were separated from each other and from mother liquor by filtration. The large crystals (180 mg, 16.6%) turned out to be the bis-prolinomethyl derivative. An analytical sample was obtained by recrystallization from EtOAc. Mp 167–170 °C. ^{1}H NMR ($CDCl_3$) δ, ppm, J, Hz: 1.58 (m, 4H), 1.85 (m, 2H), 1.92 (m, 4H), 2.23 (q, $J = 8.2$, 2H), 3.22 (dd, $J = 6$, $J = 7.8$, 2H), 3.74 (s, 6H, 2OMe), 4.04 (d, $^2J = 13.3$, 2H, $2NCH_aN$), 5.14 (d, $^2J = 13.3$, 2H, $2NCH_bN$), 7.17 (d, $^3J = 6.4$, 2H), 7.43 (m, 4H), 7.54 (d, $^3J = 6.9$, 2H). Specific rotation (c 1.9 MeCN, 25 °C) $[\alpha]_{578} = -21.9$, $[\alpha]_{546} = -18.8$, $[\alpha]_{436} = +33.4$, $[\alpha]_{406} = +81.4$, $[\alpha]_{366} = +221.3$. Circular dichroism (8.7×10^{-4} M, MeCN, cell 0.5 mm) λ_{max}, nm, ($\Delta\varepsilon$, $M^{-1}\,cm^{-1}$): 250 (15.0), 226 (7.0). Anal. Calcd for $C_{28}H_{32}N_4O_6$ (M 520.58) (%): C, 64.60; H, 6.20; N, 10.76. Found (%): C, 64.68; H, 6.47; N, 10.74.

The white powder (90 mg, mp 186–187 °C), according to ^{1}H NMR data ($CDCl_3$): 1.81 (m, 2H), 2.00 (m, 1H), 2.20 (m, 1H), 2.64 (q, $J = 7.2$, 1H), 3.05 (m, 1H), 3.56 (dd, $J = 4.8$, $J = 9.6$, 1H), 3.74 (s, 3H, OMe), 3.85 (d, $^2J = 12.3$, 1H, NCH_aN), 4.90 (d, $^2J = 12$, 1H, NCH_bN), 7.23 (d, $^3J = 7.2$, 1H), 7.26 (d, $^3J = 7.2$, 1H), 7.48 (m, 5H), 7.60 (d, $^3J = 7$, 1H), 8.31 (s, 1H, NH) seemed to be the monoprolinomethylated derivative, but exhibited no optical rotation and was not analyzed further.

4.3. Enantiomeric diphenic hydrazide (*R*)-(+)-1

Finely ground (*R*,*S*,*S*)-(+)$_{366}$-**2** (136 mg, 0.26 mmol) was suspended in aq 5% HCl (5 mL) and stirred for 12 h at 20 °C. White precipitate was collected by filtration, washed three times with 5 mL H_2O and dried in a vacuum desiccator over KOH. Yield 35 mg (56%). Mp 310 °C (dec, prior to melting aggregation of the powder was observed starting approx. at 160 °C). ^{1}H NMR (CD_3OD) similar to the racemate. Specific rotation (c 0.7 MeCN, 15 °C) $[\alpha]_{578} = 144$, $[\alpha]_{546} = 171$, $[\alpha]_{436} = 386$, $[\alpha]_{406} = 483$, $[\alpha]_{366} = 834$. Enantiomeric excess (>90%) was estimated from ^{1}H NMR with shift-reagent Eu(tfc)$_3$ ($CDCl_3$): in enantiomer for doublet at 7.27 ppm no additional splitting was observed, whereas for racemate it constituted 0.05 ppm. UV: λ_{max}, nm, (ε, $M^{-1}\,cm^{-1}$) (2.2×10^{-3} M, MeOH, cell 0.1 mm): 202.5 (3.8×10^4); (2.4×10^{-3} M, MeCN, cell 0.1 mm): 202.5 (4.7×10^4). CD λ_{max}, nm, $\Delta\varepsilon$, $M^{-1}\,cm^{-1}$ (3.5×10^{-4} M, EtOH, cell 1 mm): 241 (29.8), 221 (42); (2.2×10^{-3} M, MeOH, cell 0.1 mm): 237 (23.8), 218 (26.6); (2.4×10^{-3} M, MeCN, cell 0.1 mm): 244 (27.1), 218 (39.2). CD spectra in MeOH did not depend significantly on the temperature in the range +22 to −90 °C.

4.4. Racemization kinetics of (*R*)-(+)-1

A solution of (*R*)-(+)-**1** (c 0.2 MeCN) with measured optical rotation was divided into 5 ampoules, which were sealed and kept at (100 ± 2) °C. Every 2 h an ampoule was taken out and the optical rotation measured. $Ln(\alpha_0/\alpha)$ was plotted against time, s (6 data points). The slope constituted $k_{rac} = 2k_{enant} = (5.63 \pm 0.14) \times 10^{-5}\,s^{-1}$ ($r2 = 0.99$). $\Delta G^{\ddagger} = (126.7 \pm 0.8)$ kJ mol^{-1} was derived from $k_{enant} = (2.82 \pm 0.07)\times 10^{-5}\,s^{-1}$ and Eyring equation $k_{enant} = \kappa(k_B T/h)\,\exp(\Delta G^{\ddagger}/RT)$ where κ is the statistical factor, set equal to 2 as far as there are 2 equivalent reaction paths, k_B is the Boltzmann constant, h is Planck's constant, and R is the gas constant.

Acknowledgements

The authors thank Dr. Klaus Kolster (University Duisburg-Essen) for calculations of the electronic spectra of **1** and Prof. Paul Rademacher (University Duisburg-

Essen) for valuable discussions. This work was supported by INTAS (grant No 99-00157), the Russian Academy of Sciences (academicians Kuznetsov, Nefedov and Tartakovsky programmes) and the Russian Foundation for Basic Research (grant nos. 00-03-32738, 00-03-81187 Bel, 03-03-32019, and 03-03-06525 MAS).

References and notes

1. Bringmann, G.; Menche, D. *Acc. Chem. Res.* **2001**, *34*, 615–624, and references cited therein.
2. Hattori, T.; Shimazumi, Y.; Goto, H.; Yamabe, O.; Morohashi, N.; Kawai, W.; Miyano, S. *J. Org. Chem.* **2003**, *68*, 2099–2108.
3. Vorogushin, A. V.; Wulff, W. D.; Hansen, H.-J. *J. Am. Chem. Soc.* **2002**, *124*, 6512–6513, and references cited therein.
4. Song, Y. C.; Okamoto, S.; Sato, F. *Tetrahedron Lett.* **2002**, *43*, 8635–8637.
5. Jacobsen, E. N.; Pfaltz, A.; Yamamoto, H. *Comprehensive Asymmetric Synthesis I–III*; Springer: Berlin, 1999.
6. Takaya, H.; Ohta, T.; Noyori, R. In *Catalytic Asymmetric Synthesis*; Ojima, I., Ed.; VCH: New York, 1993; p 1.
7. Tanaka, K.; Okada, T.; Toda, F. *Angew. Chem.* **1993**, *105*, 1266–1267; *Angew. Chem., Int. Ed. Engl.* **1993**, *32*, 1147–1148.
8. Kondepudi, D. K.; Laudadio, J.; Asakura, K. *J. Am. Chem. Soc.* **1999**, *121*, 1448–1451.
9. Sakamoto, M.; Utsumi, N.; Ando, M.; Saeki, M.; Mino, T.; Fujita, T.; Katoh, A.; Nishio, T.; Kashima, C. *Angew. Chem.* **2003**, *115*, 4496–4499; *Angew. Chem., Int. Ed.* **2003**, *42*, 4360–4363.
10. Bringmann, G.; Heubes, M.; Breuning, M.; Göbel, L.; Ochse, M.; Schöner, B.; Schupp, O. *J. Org. Chem.* **2000**, *65*, 722–728.
11. Bringmann, G.; Busse, H.; Dauer, U.; Güssregen, S.; Stahl, M. *Tetrahedron* **1995**, *51*, 3149–3158.
12. Müllen, K.; Heinz, W.; Klärner, F.-G.; Roth, W. R.; Kindermann, I.; Adamczak, O.; Wette, M.; Lex, J. *Chem. Ber.* **1990**, *123*, 2349–2371.
13. Spivey, A. C.; Charbonneau, P.; Fekner, T.; Hochmuth, D. H.; Maddaford, A.; Malardier-Jugroot, C.; Redgrave, A. J.; Whitehead, M. A. *J. Org. Chem.* **2001**, *66*, 7394–7401.
14. Gawroński, J.; Grycz, P.; Kwit, M.; Rychlewska, U. *Chem. Eur. J.* **2002**, *8*, 4210–4215, and references cited therein.
15. Borecka, B.; Cameron, T. S.; Linden, A.; Rashidi-Ranjbar, P.; Sandström, J. *J. Am. Chem. Soc.* **1990**, *112*, 1185–1190.
16. Mislow, K.; Glass, M. A. W.; O'Brien, R. E.; Rutkin, P.; Steinberg, D. H.; Weiss, J.; Djerassi, C. *J. Am. Chem. Soc.* **1962**, *84*, 1455–1478.
17. Tichý, M.; Ridvan, L.; Holý, P.; Závada, J.; Císařová, I.; Podlaha, J. *Tetrahedron: Asymmetry* **1998**, *9*, 227–234.
18. Kwit, M.; Rychlewska, U.; Gawroński, J. *New J. Chem.* **2002**, *26*, 1714–1717.
19. Kostyanovsky, R. G.; Lyssenko, K. A.; Lenev, D. A.; Bronzova, I. A. *Tetrahedron: Asymmetry* **2002**, *13*, 2697–2701, and references cited therein.
20. Lenev, D. A.; Lyssenko, K. A.; Kostyanovsky, R. G. *Eur. J. Inorg. Chem.* **2003**, 2979–2985.
21. Labriola, R. A. *An. Asoc. Quim. Argent.* **1937**, *25*, 121–131; *Chem. Abstr.* **1938**, *32*, 4970.
22. Riggs, N. V.; Verma, S. M. *Aust. J. Chem.* **1970**, *23*, 1913–1917.
23. Roldan, C. M.; Brana, M. F.; Castellano, J. M.; Rabadan, F. *Arch. Farmacol. Toxicol.* **1975**, *1*, 37–42.
24. Laboratorios Made S. A., Madrid, Patent DE 2323554, 1974.
25. Rudchenko, V. F.; Chervin, I. I.; Kostyanovskii, R. G. *Bull. Acad. Sci. USSR Div. Chem. Sci. (Engl. Transl.)* **1985**, *34*, 452; *Izv. Akad. Nauk SSSR Ser. Khim.* **1985**, 494–495.
26. Etter, M. C. *Acc. Chem. Res.* **1990**, *23*, 120–126.
27. MacDonald, J. C.; Whitesides, G. M. *Chem. Rev.* **1994**, *94*, 2383–2420.
28. Shanmuga Sundara Raj, S.; Yamin, B. M.; Boshaala, A. M. A.; Tarafder, M. T. H.; Crouse, K. A.; Fun, H.-K. *Acta Cryst.* **2000**, *C56*, 1011–1012.
29. Kostyanovsky, R. G.; Lyssenko, K. A.; Kadorkina, G. K.; Lebedev, O. V.; Kravchenko, A. N.; Chervin, I. I.; Kostyanovsky, V. R. *Mendeleev Commun.* **1998**, 231–233.
30. Suzuki, H. *Electronic Absorption Spectra and Geometry of Organic Molecules*; Academic: New York, 1967.
31. Rashidi-Ranjbar, P.; Sandström, J. *J. Mol. Struct.* **1991**, *246*, 25–32.
32. Gaussian 98, Revision A.5, Frisch, M. J.; Trucks, G. W.; Schlegel, H. B.; Scuseria, G. E.; Robb, M. A.; Cheeseman, J. R.; Zakrzewski, V. G.; Montgomery, J. A., Jr.; Stratmann, R. E.; Burant, J. C.; Dapprich, S.; Millam, J. M.; Daniels, A. D.; Kudin, K. N.; Strain, M. C.; Farkas, O.; Tomasi, J.; Barone, V.; Cossi, M.; Cammi, R.; Mennucci, B.; Pomelli, C.; Adamo, C.; Clifford, S.; Ochterski, J.; Petersson, G. A.; Ayala, P. Y.; Cui, Q.; Morokuma, K.; Malick, D. K.; Rabuck, A. D.; Raghavachari, K.; Foresman, J. B.; Cioslowski, J.; Ortiz, J. V.; Stefanov, B. B.; Liu, G.; Liashenko, A.; Piskorz, P.; Komaromi, I.; Gomperts, R.; Martin, R. L.; Fox, D. J.; Keith, T.; Al-Laham, M. A.; Peng, C. Y.; Nanayakkara, A.; Gonzalez, C.; Challacombe, M.; Gill, P. M. W.; Johnson, B.; Chen, W.; Wong, M. W.; Andres, J. L.; Gonzalez, C.; Head-Gordon, M.; Replogle, E. S.; Pople, J. A. Gaussian, Pittsburgh, PA, 1998.
33. Scott, A. P.; Radom, L. *J. Phys. Chem.* **1996**, *100*, 16502–16513.
34. Mauksch, M.; Schleyer, P. v. R. *Angew. Chem.* **1997**, *109*, 1976–1980; *Angew. Chem., Int. Ed.* **1997**, *36*, 1856–1860, and references cited therein.
35. Salem, L. *Acc. Chem. Res.* **1971**, *4*, 322–328.
36. Lyssenko, K. A.; Lenev, D. A.; Kostyanovsky, R. G. *Tetrahedron* **2002**, *58*, 8525–8537.
37. Underwood, H. W., Jr.; Kochmann, E. L. *J. Am. Chem. Soc.* **1923**, *45*, 3071–3077.